



US 20010038972A1

(19) United States

(12) Patent Application Publication

LYONS et al.

(10) Pub. No.: US 2001/0038972 A1

(43) Pub. Date: Nov. 8, 2001

(54) ULTRA-THIN RESIST SHALLOW TRENCH  
PROCESS USING METAL HARD MASK

(22) Filed: Nov. 20, 1998

(75) Inventors: CHRISTOPHER F. LYONS,  
FREMONT, CA (US); SCOTT A.  
BELL, SAN JOSE, CA (US); HARRY  
J. LEVINSON, SARATOGA, CA  
(US); KHANH B. NGUYEN, SAN  
MATEO, CA (US); FEI WANG, SAN  
JOSE, CA (US); CHIH YUH YANG,  
SAN JOSE, CA (US)

Publication Classification

(51) Int. Cl. 7 ..... G03C 5/00; G03F 7/00;  
H01L 21/76

(52) U.S. Cl. ..... 430/313; 430/311; 430/316;  
430/423; 430/424; 430/432

(57) ABSTRACT

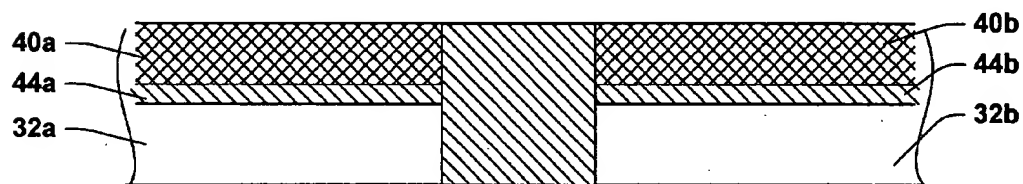
A method of forming a shallow trench isolation is provided. In the method, a barrier oxide layer is formed on a substrate, and a silicon nitride layer is formed on the barrier oxide layer. A metal layer is formed on the silicon nitride layer, and an ultra-thin photoresist is formed on the metal layer. The ultra-thin photoresist layer is patterned with short wavelength radiation to define a pattern for a shallow trench. The ultra-thin photoresist layer is used as a mask during a first etch step to transfer the shallow trench pattern to the metal layer. The first etch step includes an etch chemistry that is selective to the metal layer over the ultra-thin photoresist layer. The metal layer is used as a hard mask during a second etch step to form the shallow trench by etching portions of the silicon nitride layer, barrier oxide layer and substrate.

Correspondence Address:  
AMIN & TUROCY, LLP  
1900 EAST 9TH STREET, NATIONAL CITY  
CENTER  
24TH FLOOR,  
CLEVELAND, OH 44114 (US)

(73) Assignee: Christopher F. Lyons

(\*) Notice: This is a publication of a continued prosecution application (CPA) filed under 37 CFR 1.53(d).

(21) Appl. No.: 09/197,383



*Hand made thin resist  
unexpected results*

# Tungsten patterning for 1:1 x-ray masks

C. W. Jurgensen, R. R. Koia, A. E. Novembre, W. W. Tai, J. Frackoviak, L. E. Trimble, and G. K. Celler  
AT&T Bell Laboratories, 6F325, Murray Hill, New Jersey 07974

(Received 10 June 1991; accepted 11 July 1991)

A subtractive process to form subhalf micron, vertical-walled patterns in half-micron thick tungsten on x-ray masks has been developed. Electron-beam lithography was used to form resist patterns on a structure consisting of 300 Å Cr on 5000 Å W on 200 Å Cr on an approximately 1  $\mu\text{m}$  thick poly-silicon or silicon nitride membrane. The Cr masking and etch-stop layers above and below the W layer are required because the resist and membrane materials etch rapidly in fluorine based W etching plasmas. Chromium was chosen for these layers because it has a high selectivity in the W etch ( $\approx 40:1$ ), is compatible with the W deposition process, and can be patterned in an  $\text{O}_2\text{-Cl}_2$  plasma which does not etch W or the membrane materials. Helium backside cooling at a pressure from 1 to 5 Torr controls membrane temperature during all plasma processing steps. Pure  $\text{CBrF}_3$ , or  $\text{CHF}_3$ , etch W slowly while simultaneously depositing polymer which produces sloping profiles where the base of the feature is wider than the initial mask width. Pure  $\text{SF}_6$  gives high etching rates but the fluorine radicals attach the W sidewall causing undercutting. Depositing polymer on the sidewall by adding  $\text{CHF}_3$  or  $\text{CBrF}_3$  to the  $\text{SF}_6$  reduces undercutting, but produces sloping profiles. The undercutting found with pure  $\text{SF}_6$  can be eliminated with vertical profiles by etching at low temperature or by adding  $\text{N}_2$  or  $\text{Cl}_2$  to the gas mixture to form low volatility reaction products with tungsten on the sidewall.

## I. INTRODUCTION

X-ray lithography has long been a candidate to replace optical lithography; however continuing progress in optical lithography ensures that it will remain the dominant technology through the 0.35  $\mu\text{m}$  device generation. X-ray lithography is now being targeted for 0.25  $\mu\text{m}$  lithography, but pattern placement accuracy, feature size control, metrology, defect inspection, and defect repair are formidable difficulties in fabrication of 0.25  $\mu\text{m}$  1:1 x-ray masks. For example, the standard deviation of feature size on the mask must be less than 50 Å to meet a three sigma specification of 0.03  $\mu\text{m}$  for patterns on the product wafer assuming that errors add in quadrature and that the wafer etch process, resist process, exposure tool, and mask are each allocated equal contributions to the error budget. To date the best reported linewidth control on an x-ray mask is  $\sigma = 80$  Å on 0.5  $\mu\text{m}$  gold absorber lines.<sup>1</sup> The wall angle in a half-micron thick absorber layer must be within 0.3° of vertical to hold a 50 Å linewidth difference between the top and bottom of the absorber layer. Metrology is a significant issue<sup>2</sup> for 0.25  $\mu\text{m}$  masks because the measurement precision on state of the art scanning electron micrograph (SEM) metrology systems is comparable to the linewidth control requirement.

Two absorber technologies are currently being evaluated for x-ray masks. Gold absorber patterns produced by an additive electroplating process<sup>3-5</sup> have the advantage of low absorber stress and reduced proximity effects.<sup>6</sup> Tungsten or tantalum absorber patterns produced by subtractive etching process<sup>7,8</sup> are attractive because these materials are thermally stable, have a close expansion match with Si and mask materials, and are deposited and etched with standard very large scale integrated (VLSI) processing methods. Karnezos *et al.*<sup>7</sup> used tri-layer lithography to obtain half-micron tungsten patterns; however, this process is unlikely to provide the required linewidth control because it involves three

sequential etch steps where the final step has a poor selectivity for etching tungsten relative the organic mask. Two studies<sup>9,10</sup> have demonstrated 0.1  $\mu\text{m}$  tungsten patterning using a nickel etch mask which was patterned by the lift-off method. These results<sup>9,10</sup> are promising, but improvements in profile control are required to reduce the width difference between the top and bottom of the W layer from about 500 Å in these studies. It is also important to determine if an etching process produces satisfactory profiles and linewidth control for both isolated and array type features. Finally the lift-off patterning method used in these studies<sup>9,10</sup> is not useful for x-ray mask fabrication because it results in high defect densities. In this paper we describe W patterning processes that overcomes several of the disadvantages discussed above.

## II. MASK STRUCTURE

Our preferred mask structure consists of a polycrystalline Si membrane<sup>11</sup> which is deposited directly on an optically flat mask blank machined of fused silica or glass. A wet etch releases the membrane. An rf sputtering process is then used to deposit 200 Å of low stress CR which functions as an etch stop for the W etch. A 5000 Å thick layer of low stress  $\alpha$  phase W absorber is then deposited in the same sputtering system.<sup>12</sup> Finally, 300 Å of low stress Cr is deposited as a pattern transfer layer. This structure is coated with an e-beam resist, exposed, and developed. The resist pattern is transferred into the Cr transfer layer with an  $\text{O}_2\text{-Cl}_2$  plasma and the resulting pattern is transferred into the W layer with a fluorine based plasma. Note that no resist stripping process is required because all the resist is consumed during the W etching step. Finally the pattern is transferred through the Cr etch stop layer to allow optical alignment through the membrane. The same process sequence may also be applied to  $\text{Si}_x\text{N}_y$  membranes.

# Shipley SAL® 601 on Cr/W/Cr/Si

1/2  $\mu\text{m}$  L/S at 8  $\mu\text{C}/\text{cm}^2$

initial

after Cr etch

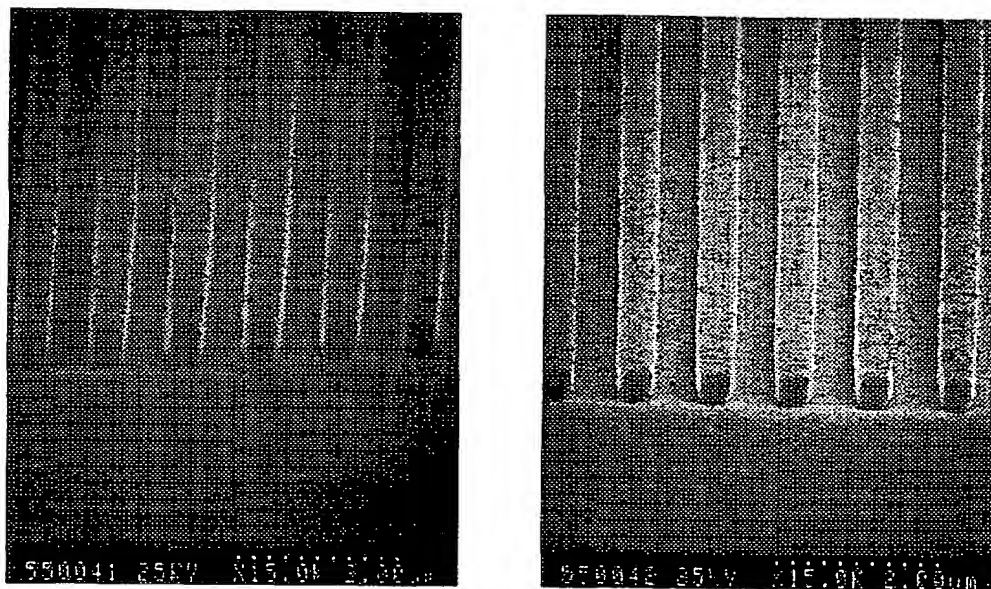


FIG. 1. A grouping of half-micron lines and spaces on a Cr/W/Cr coated Si wafer are shown before and after the Cr etch.

### III. ELECTRON-BEAM LITHOGRAPHY

Electron-beam exposures were performed at 40 keV on a Cambridge EBMF 10.5 Vector scan system set to 1 nA beam current, and 90 nm spot size. Two negative acting e-beam resist were studied: Shipley SAL® 601, and poly (trimethylsilylmethyl methacrylate-co-3, 4-chloromethylstyrene) [P(SI-CMS)].<sup>13</sup> Figure 1 shows half micron line and space patterns in Shipley SAL® 601 resist exposed without proximity correction at 8.0  $\mu\text{C}/\text{cm}^2$  on Cr/W/Cr coated Si wafer. Similar results are obtained on Cr/W/Cr coated membranes; however, we can not mount large membranes in our SEM at the 80° viewing angle shown in Fig. 1. The right-hand side of Fig. 1 shows the resist features after Cr etch in a 1:1 Cl<sub>2</sub>-O<sub>2</sub> mixture at 90 mTorr. For this etching condition, the resist thickness loss was over 1000 Å and there was about 100 Å of undercutting in the Cr layer. The Cr etching process has not been optimized for linewidth control, but we have found that the conditions which optimize selectivity (high pressure, low bias) result in isotropic Cr etching with several hundred angstroms of linewidth loss.

Figure 2 shows half- $\mu\text{m}$  L/S patterns in P(SI-CMS) exposed at 5.5  $\mu\text{C}/\text{cm}^2$  on Cr/W/Cr coated Si wafer. At low post develop bake temperature, the patterns have rough sidewalls and an apron of residual resist at the base of the feature, while the resist flows at higher bake temperature

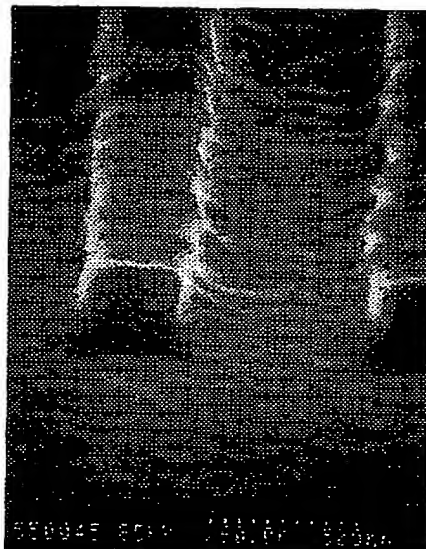
resulting in smoother edges and shallow sidewall angles. Figure 2(b) shows that in spite of the shallow sidewall angle, this resist (baked at 105 °C) can be used to transfer patterns into the Cr layer and ultimately produce tungsten patterns with vertical sidewalls. This is possible because P(SI-CMS) is a high selectivity mask for Cr, and Cr is a high selectivity mask for W. The mechanism for this high selectivity is a reaction between oxygen and the silicon contained in the resist to form a protective SiO<sub>2</sub> layer on the resist surface in the O<sub>2</sub>-Cl<sub>2</sub> plasma. Figure 3 shows a top down view of half and quarter micron features on a membrane which were obtained with the P(SI-CMS) resist and transferred into 5000 Å of tungsten. The edge roughness seen in Fig. 3 was present on the resist lines and is not a result of the etching process.

Without proximity correction we have observed that coded 0.5  $\mu$  isolated resist lines print up to 3000 Å narrower than lines adjacent to 10  $\mu\text{m}$  wide pads on Cr/W/Cr coated membranes. We have not yet determined if proximity correction can give the two orders of magnitude improvement in resist linewidth control which is required to make direct e-beam writing viable for subtractive x-ray mask fabrication schemes.

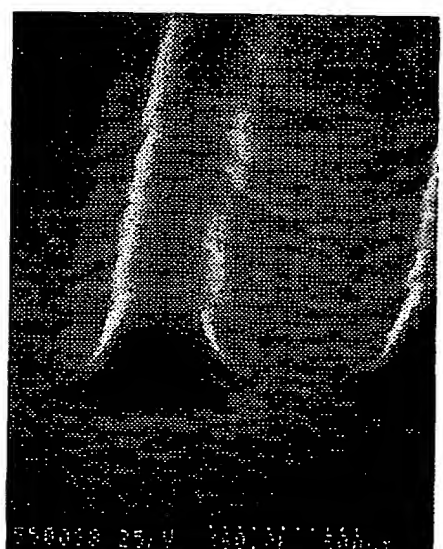
### IV. MEMBRANE TEMPERATURE CONTROL

In preliminary etching evaluations we did not attempt to control membrane temperature during etching; however we

**Si-CMS ON Cr/W/Cr/Si**  
**1/2  $\mu$ m L/S 5.5  $\mu$ C/cm<sup>2</sup>**



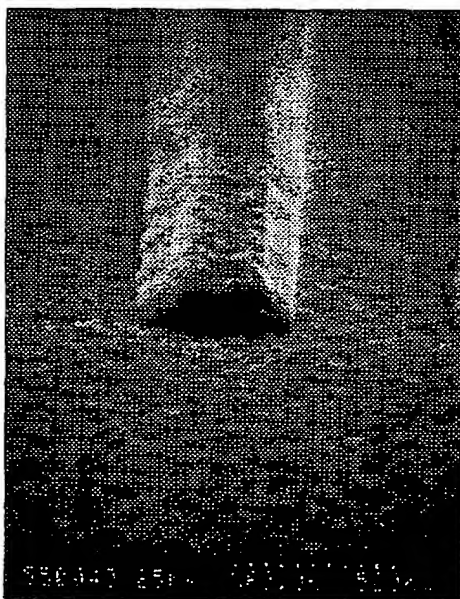
**90°C BAKE**



**105°C BAKE**

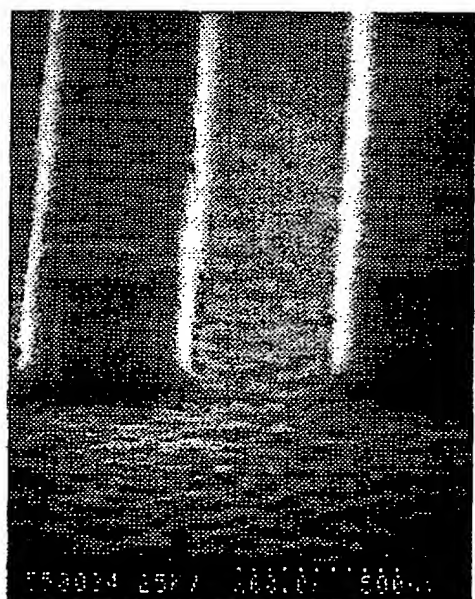
**1/2  $\mu$ m L/S**

**AFTER CHROME ETCH**



**1:1 O<sub>2</sub> - Cl<sub>2</sub>**

**AFTER TUNGSTEN ETCH**



**1:1 SF<sub>6</sub> - CBrF<sub>3</sub>**

FIG. 2. A half-micron P(Si-CMS) array line is shown as it appears through four stages of the tungsten patterning sequence.

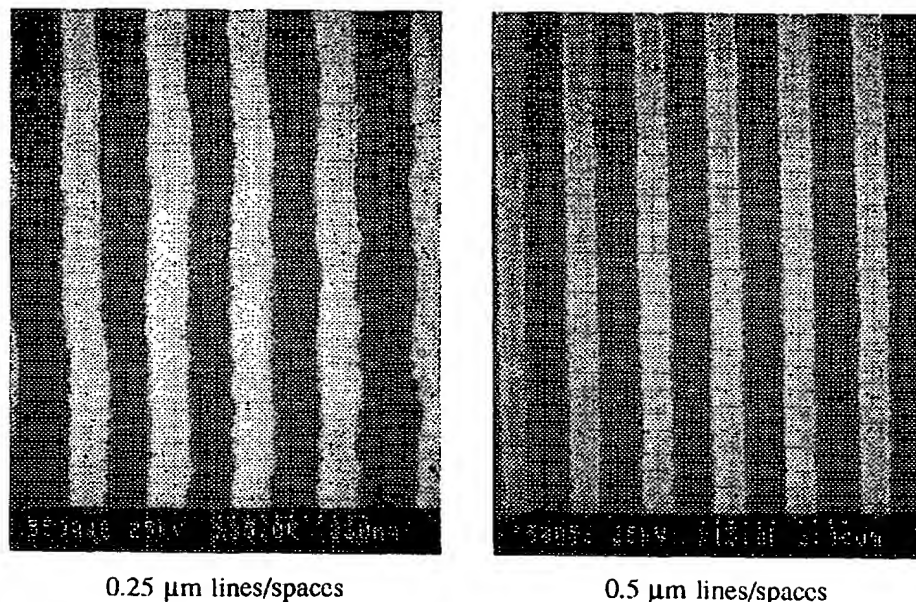
5000Å TUNGSTEN FILM AFTER ETCHING IN  $\text{CBrF}_3$ - $\text{SF}_6$ .

FIG. 3. Half- and quarter-micron features obtained with P(Si-CMS) resist on a membrane are shown after pattern transfer into 5000 Å of tungsten.

observed resist degradation, severe undercutting, and etching rates which differed from results obtained on wafer samples. These problems were eliminated with helium backside cooling at pressure from 1 to 5 Torr and a membrane to

electrode gap of about 100  $\mu\text{m}$ . With helium backside cooling we have not observed any difference between etching results on membrane samples and wafer samples. The SEMs shown in the remainder of this paper are all on wafer samples

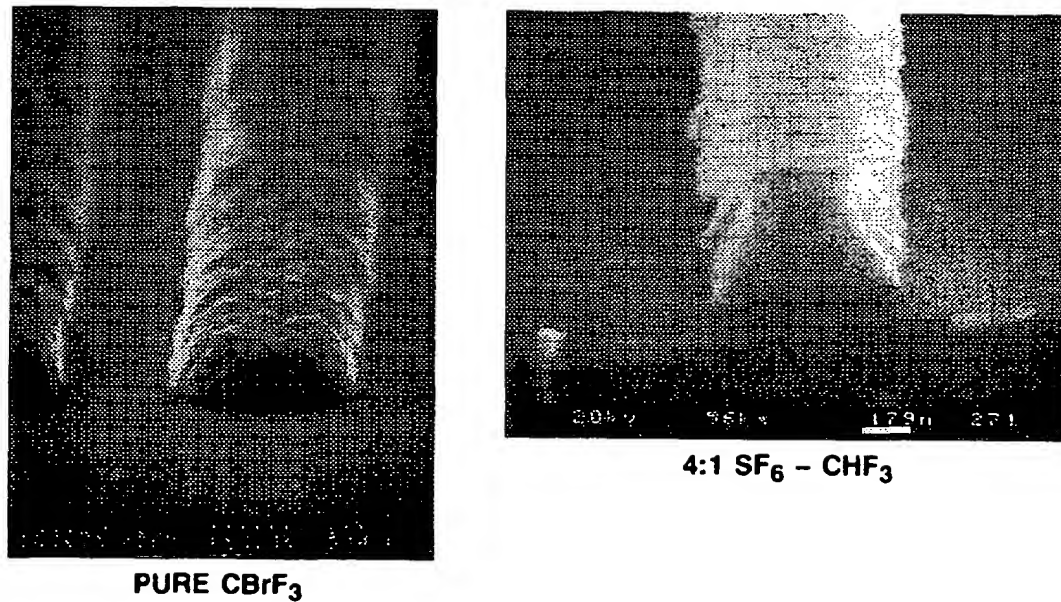
1/2  $\mu\text{m}$  L/S AFTER TUNGSTEN ETCH

FIG. 4. This figure shows some problems we encountered using gas mixtures and etch processes similar to those recommended in previous studies (Refs. 9 and 10).

because these samples can be cleaved and tilted to high viewing angles to reveal profile information.

#### V. TUNGSTEN ETCH PROFILES

All W etching experiments described here were performed in the reactive ion etching (RIE) mode of a custom built etcher with a 114 mm diam powered electrode. A 7 mm thick dielectric clamp ring confined the densest part of the plasma to a 75 mm diam disk directly over the mask substrate. The center of the electrode has a 26 mm diam by 4.5 mm high raised region, which results in an electrode to membrane gap of about 0.1 mm when a mask substrate is clamped into place. An additional support ring was used to allow 75 mm wafer samples to be etched in this system with the same wafer to electrode gap. The etching results presented here were obtained at 27 MHz, 5 mTorr, 20–50 sccm total flow rate, backside He pressure from 0 to 5 Torr, and 20 W incident power which results in a self-bias of 100 to 150 V. Profiles were examined after 10–25% overetch based on etching rates determined by laser reflectance endpoint on unpatterned W coated wafers. No loading effects or dependence of etching rates on trench aspect ratio were observed for aspect ratios up to two.

Figure 4 shows the W etching results obtained on wafer samples without He cooling using the  $\text{CBrF}_3$  plasma,<sup>9</sup> and a 4:1  $\text{SF}_6$ – $\text{CHF}_3$  mixture.<sup>10</sup> We observed  $\approx 2000 \text{ \AA}$  of undercutting in the 4:1  $\text{SF}_6$ – $\text{CHF}_3$  mixture, however, this undercutting was reduced to  $\approx 300 \text{ \AA}$  with 1 Torr of He and an electrode temperature of 20 °C. These results suggest that Tennant *et al.*<sup>10</sup> heat sunk their samples to the electrode. Pure  $\text{CBrF}_3$  resulted in complete erosion of the Cr masking

layer and loss of nearly half the thickness of the W layer. Pure  $\text{CBrF}_3$  also produced sloping sidewalls where the base width is  $\approx 1500 \text{ \AA}$  wider than the initial width of the Cr mask. We also observed that lines in a line-space array had steeper sidewalls and less linewidth growth at the base than isolated lines. These results are consistent with a profile evolution model<sup>14</sup> where etching is accompanied by an isotropic angular distribution of depositing particles with a sticking coefficient of one. In this model, the dependence on the proximity of neighboring lines results from shadowing, which predominantly affects the isotropic angular distribution of depositing particles. This effect is also observed to a lesser extent in a 1:1  $\text{CBrF}_3$ – $\text{SF}_6$  mixture at 20 °C and 1 Torr He as shown in Fig. 5. Here the Cr mask is intact and the array features have nearly vertical sidewalls, but the isolated line has sloping sidewalls with a base width  $\approx 500 \text{ \AA}$  wider than the width of the Cr mask.

Figure 6 shows the effect of electrode temperature on undercutting in pure  $\text{SF}_6$  at a helium backside pressure of 5 Torr. At 20 °C the undercut is  $\approx 400 \text{ \AA}$  while at –20 °C the undercut is less than 200  $\text{\AA}$  and nearly vertical profiles are obtained for both isolated and array lines. Undercutting can also be eliminated by reactions which form low volatility products on the side walls, as shown in Fig. 7, where the etching was done at 20 °C and 5 Torr He on the backside. The 1:1  $\text{SF}_6$ – $\text{Cl}_2$  mixture resulted in complete erosion of the Cr masking layer and  $\approx 1500 \text{ \AA}$  thickness loss of the W layer, but preserved vertical profiles with the initial width of the Cr mask. The Cr mask is intact for the 1:1  $\text{SF}_6$ – $\text{N}_2$  mixture which produces nearly vertical sidewalls with no undercutting.

#### 5000 Å TUNGSTEN FILM AFTER ETCHING IN $\text{CBrF}_3$ – $\text{SF}_6$ .

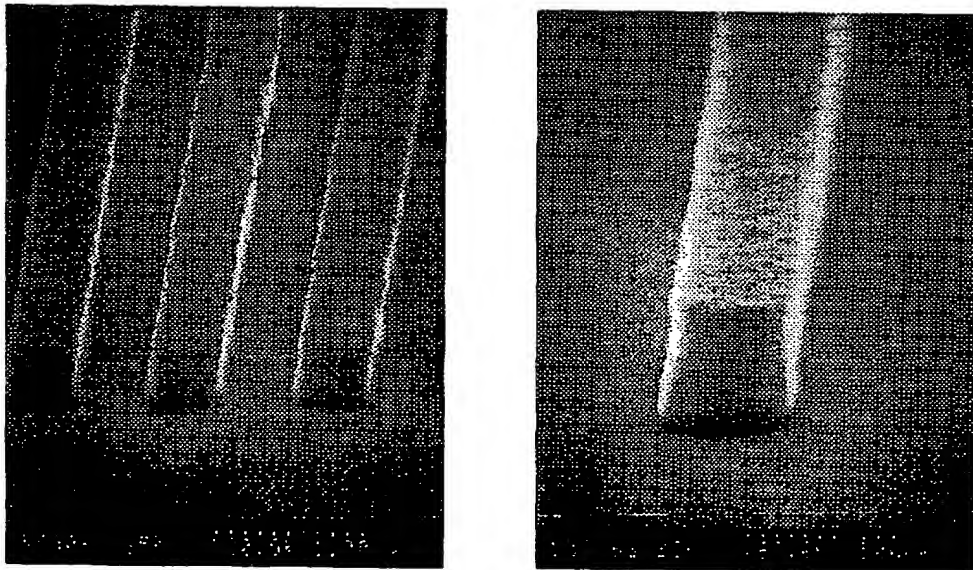


FIG. 5. Polymer deposition can cause sloping sidewalls and linewidth growth for isolated lines while still producing vertical profiles for densely packed lines.

### profile in pure SF<sub>6</sub> plasma

-20 °C

20 °C

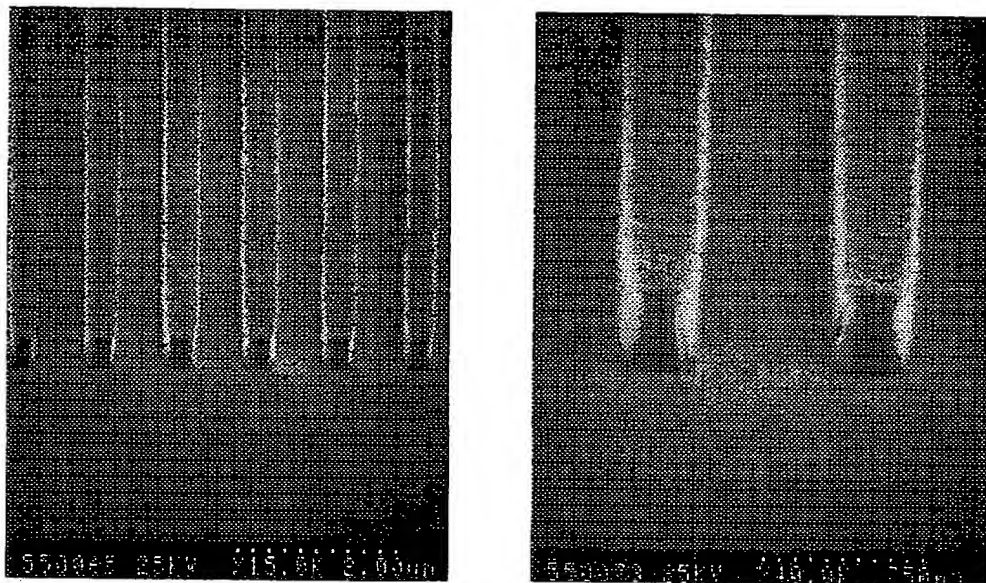


FIG. 6. In pure SF<sub>6</sub> there is about 400 Å of undercut at 20 °C and less than 200 Å of undercut at -20 °C.

## Reactive blocking of undercutting

1:1 N<sub>2</sub>-SF<sub>6</sub>

1:1 Cl<sub>2</sub>-SF<sub>6</sub>

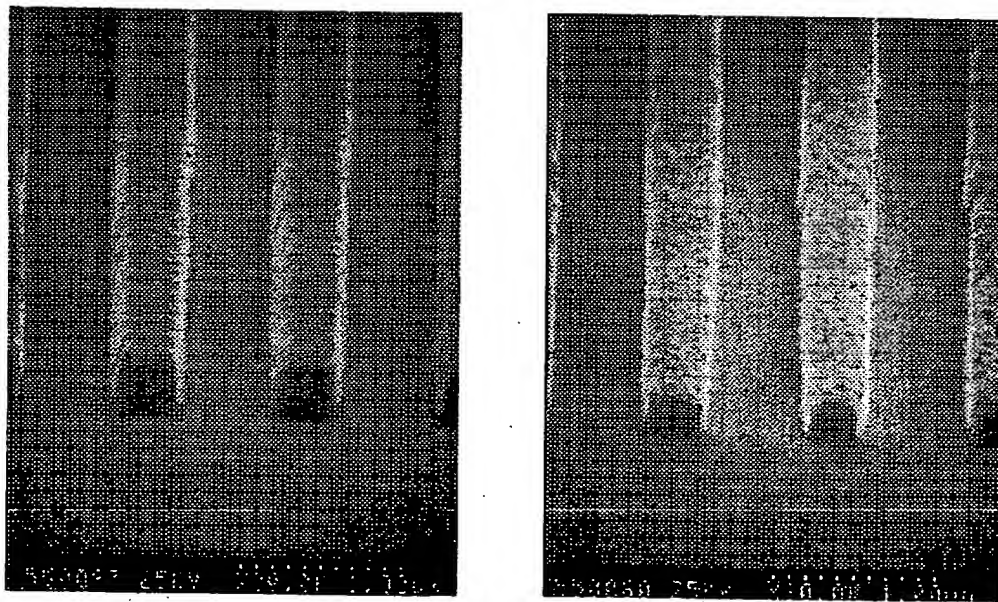


FIG. 7. Undercutting can also be eliminated by adding  $N_2$  or  $Cl_2$  to the gas mixture because these gases react to form low volatility products on the sidewall.

## VI. CONCLUSIONS

We have shown that sub-half micron vertical walled features can be etched into 0.5  $\mu\text{m}$  thick tungsten absorber layers on membranes for 1:1 x-ray mask applications. Helium backside cooling to maintain membrane temperature control is required to obtain anisotropic etching results. Undercutting can be eliminated by etching at temperatures less than  $-20^\circ\text{C}$  or by chemical sidewall protection. Depositing polymer on the sidewall by adding  $\text{CHF}_3$  or  $\text{CBrF}_3$  to the gas mixture reduces undercutting, but for isolated lines it produces sloping profiles and linewidth growth. Chromium may be applied in the same deposition system as tungsten and is useful as an etch stop layer and as a pattern transfer masking layer. Finally, direct e-beam writing for subtractive x-ray mask schemes will require proximity correction and high contrast resists.

<sup>1</sup>J. Warlaumont, *J. Vac. Technol. B* **7**, 1634 (1989).

<sup>2</sup>G. O. Foss, *J. Vac. Sci. Technol. B* **8**, 2028 (1990).

- <sup>3</sup>G. E. Georgiou, C. A. Janoski, and T. A. Palumbo, *Proc. SPIE* **471**, 96 (1984).
- <sup>4</sup>R. E. Acosta, A. D. Wilson, and J. V. Powers, in *Microelectronic Engineering* (North-Holland, Amsterdam, 1985), pp. 573-579.
- <sup>5</sup>G. Hughes, G. Doyle, G. Foss, and N. Gorbachenko, *J. Vac. Sci. Technol. B* **7**, 1570 (1989).
- <sup>6</sup>M. G. Rosciold, S. A. Rishton, D. P. Kern, D. E. Seeger, and C. A. B **5**, 283 (1987).
- <sup>7</sup>M. Karnezos, R. Ruby, B. Heflinger, H. Nakano, and R. Jones, *J. Vac. Sci. Technol. B* **5**, 283 (1987).
- <sup>8</sup>M. Yamada, K. Kondo, M. Nakaishi, J. Kudo, and K. Sugishima, *J. Electrochem. Soc.* **137**, 2231 (1990).
- <sup>9</sup>M. L. Schattenburg, I. Plotnik, and H. I. Smith, *J. Vac. Sci. Technol. B* **3**, 272 (1985).
- <sup>10</sup>D. M. Tenant, S. C. Shunk, M. D. Feuer, J. M. Kuo, R. E. Behringer, T. Y. Chang, and R. W. Epworth, *J. Vac. Sci. Technol. B* **7**, 1836 (1989).
- <sup>11</sup>L. E. Trimble and G. K. Celler, *J. Vac. Sci. Technol. B* **7**, 1675 (1989).
- <sup>12</sup>R. R. Kola, G. K. Celler, J. Frackoviak, C. W. Jurgensen, and L. E. Trimble, *J. Vac. Sci. Technol. B* **9**, 3301 (1991).
- <sup>13</sup>A. E. Noveembre, M. J. Jurek, A. Kornblit, and E. Reichmanis, *Poly. Eng. Sci.* **29**, 920 (1989).
- <sup>14</sup>Unpublished results based on E. S. G. Shaqfeh, and C. W. Jurgensen *J. Appl. Phys.* **66** 4664 (1989).

# The Feasibility Study of Thin Cr Film for Low Process Bias

*Woong-Won Seo, Si-Yeul Yoon, Dong-il Park, Eui-Sang Park,  
Jin-Min Kim, Sung-Mo Jeong, Sang-Soo Choi  
Han-Sun Cha\*, Kee-Soo Nam\**

*Photomask R&D center, Photronics-PKL  
493-3, Sungsung, Cheonan, 330-300, Korea  
\* S&S Tech., 9 Horim, Dalseo, Daegu, 704-240, Korea  
Phone: 82-41-559-0787, Fax: 82-42-559-0784, E-mail: wwseo@pkl.co.kr*

## ABSTRACT

As minimum feature size of device shrink down below 100 nm, the process margin for the mask fabrication reduced dramatically. Mask makers are enlisting equipment and material suppliers in their efforts to achieve wide process margin from existing processes. One of the most promising methods is thinning Cr thickness as low as possible. However, bringing the thin Cr blank into mass production line could cause some problem for advance photomask fabrication using 50 kV electron beam writing tools. In this paper, we verified the feasibility of Cr film ranged from 400 Å to 1000 Å. The results categorized into two sections. At first, we verified the writing property change with thinning Cr thickness and then investigated the etching characteristics. As a result, we found that Cr thickness don't affect writing properties regardless of Cr thickness. However, the thinner Cr blank represented superior etching characteristics to a conventional one. It showed low etching bias and loading effects. From these results, we concluded the thinner Cr blank could not only make the process wider but also improve the mask quality.

**Keywords :** thick, thin and thinner Cr film blanks, etching bias, process margin, linearity

## 1. INTRODUCTION

The complexity of the mask-making process has increased dramatically in the past few years and will continue to become more challenging as dimensions and error budgets continue to contract. The causes of mask CD (Critical Dimension) errors have three primary sources: the process (develop, etch), the writing tool and the blanks. Over the past few years, the mask industry has been focused on migrating to dry-etch processes in order to obtain better CD control

for the Cr patterning. To achieve better resolution and to improve the CD uniformity, photomask manufacturing adapted higher-energy e-beam exposure systems. In addition to the above efforts, mask makers are enlisting material suppliers in their efforts to achieve wide process margin from existing processes.

One approach to improve the blank quality is reducing Cr thickness. This will reduce etch bias between before and after the dry etch process. As a result, we could have wider process margin that we could make additional developing or etching to reduce the unetched Cr remain. It also improves the pattern fidelity that the improvement of aggressive OPC (Optical Proximity Correction) pattern is expected. Some results indicated that a thinner Cr film improved CD linearity.

However, the introduction of 50 kV e-beam writer made mask-making process more complex. As acceleration voltage became high up to 50 kV, the incident electron beam penetrates the Cr film and it is scattered both elastically and inelastically. Consequently, the incident electrons will spread out as they penetrate until all energy is lost or get out of the solids as a result of backscattered deflections. These could affect DICD (Develop Inspection Critical Dimension). Therefore, we investigate the DICD trend with changing dose and  $\eta$  (back scattering ratio) values.

After verifying writing properties, we studied dry etching characteristics of thin Cr blank. There are so many studies on the dry etch process to minimize loading effect and to get wider process margin. However, there is some trade offs between loading effect and process margin. Some recipe could improve loading effect on the exposure of reducing process margin. Or the contrary is possible. However, reducing Cr film thickness could improve both process margin and loading effect.

In this paper, we present the effects of Cr thickness on writing properties and etching process during mask fabrication process by evaluating thinner Cr film against conventional Cr film.

## 2. EXPERIMENTAL

This study was performed on an advanced tool sets comprising of a 50 kV e-beam writer EBM-3500B, PKL dry etcher CP6000U, and HOLON CD-SEM EMU-300. Table 1 shows 3 types of binary for this study. Cr thickness ranged from 400 Å to 1000 Å. All of the blanks were coated with positive CAR (Chemically Amplified Resist), FEP-171. The blanks used in this work are 6 inch square area and 250 mil thickness supplied by S&S Corporation. All exposures were done with EBM-3500B and its acceleration voltage is 50 kV. After investigating the exposure characteristics, the optimal dose was applied to process. Then the patterns etched with the Cl<sub>2</sub>/O<sub>2</sub>/He plasma in dry etch system. All process tool were shown in Table 2. Table 3 shows evaluation items for writing and etching characteristics. The test patterns used for this study are shown in figure 1. Pattern in figure 1(b) is used for backscattering ratio and dose sensitivity and patterns in figure 1(c) are used for loading effect verification. The loading effect was characterized from the data obtained by point-by-point subtraction between FICD (Final Inspection Critical Dimension) and DICD.

**Table 1. Blank specification**

	Type A	Type B	Type C
P/R (Å)	FEP-171 (3000)		
Cr thickness (Å)	400	660	1000

**Table 2. Process tools**

Process	Tool
EB Writing	EBM-3500B
PEB	ASB-5000
Development	ASP-5000
Dry etching	CP6000U
CD measurement	CD-SEM

**Table 3. Evaluation items**

Items	Contents
Dose sensitivity	CD range of dose from 9 $\mu\text{C}/\text{cm}^2$ to 13 $\mu\text{C}/\text{cm}^2$ for three samples
PEC parameters	Backscattering ratio: $\eta$ , Backscattering width : $\sigma$
CD linearity	CD range of space pattern from 0.3 $\mu\text{m}$ to 1.5 $\mu\text{m}$
Loading effect	CD range of 1.0 $\mu\text{m}$ space pattern on the distance from 1.0 $\mu\text{m}$ to 25.0 $\mu\text{m}$
Pattern profile	CD range of contact pattern from 0.2 $\mu\text{m}$ to 0.8 $\mu\text{m}$

### 3. RESULTS AND DISCUSSIONS

#### 3.1 Writing properties

##### 3.1.1 Dose sensitivity

Figures 2(a) and 2(c) show DICD of type A and type C, respectively. From the graph, we obtained approximately similar DICD with different Cr film thickness. CD variation is about 20 nm/dose for three samples. The etching bias of type A was 13.0 nm and that of type C was 39.7 nm. From these results, we found that dose sensitivity is independent on the Cr thickness. Therefore, we applied same dose for the pattern generation regardless of Cr thickness.

### 3.1.2 PEC parameters

To check Cr thickness effects on pattern generation, we adopted the PEC (Proximity Effect Correction) factors. The PEC are classified to backscattering ratio ( $\eta$ ) and backscattering width ( $\sigma$ ). The backscattering coefficient is defined a ratio of the number of backscattered electrons to incident electrons. The optimization for the correction parameters is fixed process conditions for each blanks. The values of  $\eta$  and  $\sigma$  can be changed in a reticle by the unit of drawing group. Therefore, these are the function to determine the optimum correction parameter. Figure 2(a) and 2(c) imply that  $\eta$  and dose value change didn't make any differences. PEC parameters are not influenced by Cr film thickness. Moreover, the CD difference between various type of pattern density was minimized at the same PEC value regardless of Cr film thickness. In other words, Cr thickness do not seriously affect the electron scattering. So we used same condition for pattern generation in this study.

## 3.2 Etching properties

### 3.2.1 Linearity of etching bias

The test pattern used for the linearity of etching bias was represented in figure 1(b). The results are shown in figure 3, where linearity trend for the patterns larger than 1.0 um space CD represented similar trends. However, at the pattern below 0.2 um, etching bias trends did not vary with the Cr film thickness. However, Cr film became thinner, etching bias decreased more abruptly. The etching bias range of type A, B, and C were 8.4 nm, 10.5 nm, and 11.9 nm respectively. This etching bias difference generated by Cr thickness is believed to have so-called, 'loading effects'. As space pattern decreased, the aspect ratio became so high that the by-product remained bottom of the space pattern and won't be removed easily. These hinder diffusion of radicals that the local depletion of etchant species occurs. So these phenomena could be minimized by reducing aspect ratio of target pattern like applying for a thinner Cr.

### 3.2.2 Loading effect

The loading effect was mainly originated from dry etch and the dry etch contribution of CD uniformity could be obtained by FICD-DICD. CD values for loading effect were obtained in the pattern as shown figure 1(c). We measured 1.0 um space CD pattern to find out etching bias dependency on the pattern density. The results are shown in figure 4(c). The etching bias ranges of type A, B, and C were 3.4 nm, 6.9 nm, and 10.4 nm, respectively. Although Type A, B and C have same pattern density, they have different etching time. The etching time of type A, B, and C were 300 sec, 354 sec and 423 sec, respectively. These time difference made CD difference.

## 3.3 Pattern fidelity

The contact hole patterns of type A, B, and C are shown in the figure 5. From the result, we found that decreasing Cr thickness had improved pattern fidelity. The thinner Cr thickness become, the smaller the etch bias become and pattern fidelity is strongly related with the etch bias. Therefore thinner Cr showed best pattern fidelity of the three samples in terms of anisotropic etching rate.

#### 4. CONCLUSIONS

To get a wider process margin, this study was to decreased Cr film thickness. In respect to exposure, PEC parameters are not influenced by Cr film thickness. The PEC factors of CD variations were stabilized at a range from 400 Å to 1000 Å for Cr film thickness. In respect to etching bias, the thicker the film to be etched, the worse is the etch bias and process tolerance. On the other hand, the thinner the film is the better that. Consequently, thinner Cr film blanks have capability to minimized process bias enough to produce fine features. It is concluded that thinner Cr had lower etch bias, good linearity and good uniformity than thick Cr. Therefore, we had better use thinner Cr in order to improve reticle CD accuracy.

#### 5. ACKNOWLEDGMENT

The authors would like to thank S&S Corporation for supplying blanks.

#### REFERENCES

1. Y. Sato, H. Handa, "Process bias control with thin Cr film blanks for 90nm-node reticle fabrication" Proc SPIE, Vol. 4889, P.50, 2002.
2. B.C. Cha, S.W. Choi, J.M. Kim, "Resolution Enhancement with Thin Cr for Chrome Mask Making" Proc SPIE, Vol. 2793, P.53, 1996.
3. M. Kurihara, T. Segawa, D. Okuno, N. Hayashi and H. Sano, "Performance of a Chemically Amplified Positive Resist for Next Generation Photomask Fabrication." Proc SPIE, Vol.3226, P.82, 2001.
4. Christopher Magg, Michael Lercel, "Evaluation of an advanced chemically amplified resist for next generation lithography mask fabrication" Proc. SPIE, Vol.4186, P.707, 2001.
5. H. Handa, S. Yamauchi, "Dry etching technology of Cr films to produce fine pattern reticles under 720 nm with ZEP-7000" Proc. SPIE, Vol.3873, P.98, 1999.

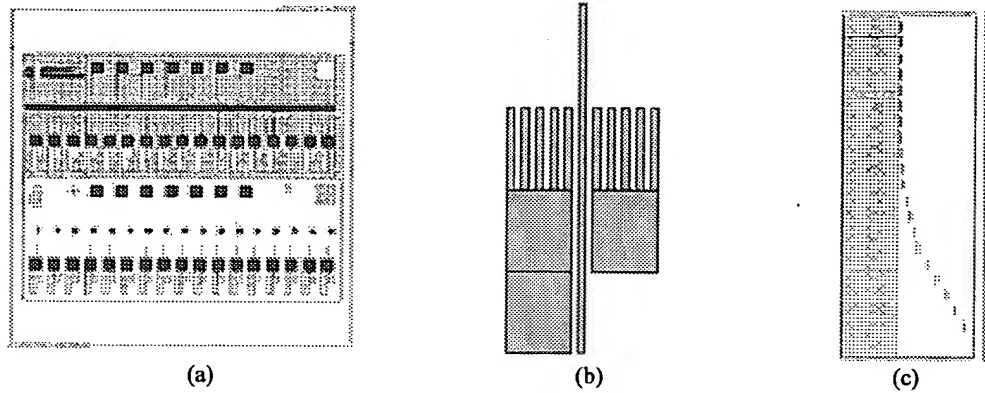


Fig 1. Experimental layout.

(a) Layout, (b) Backscattering ratio pattern (0.5  $\mu\text{m}$  space), and (c) Backscattering width pattern (1.0  $\mu\text{m}$  space).

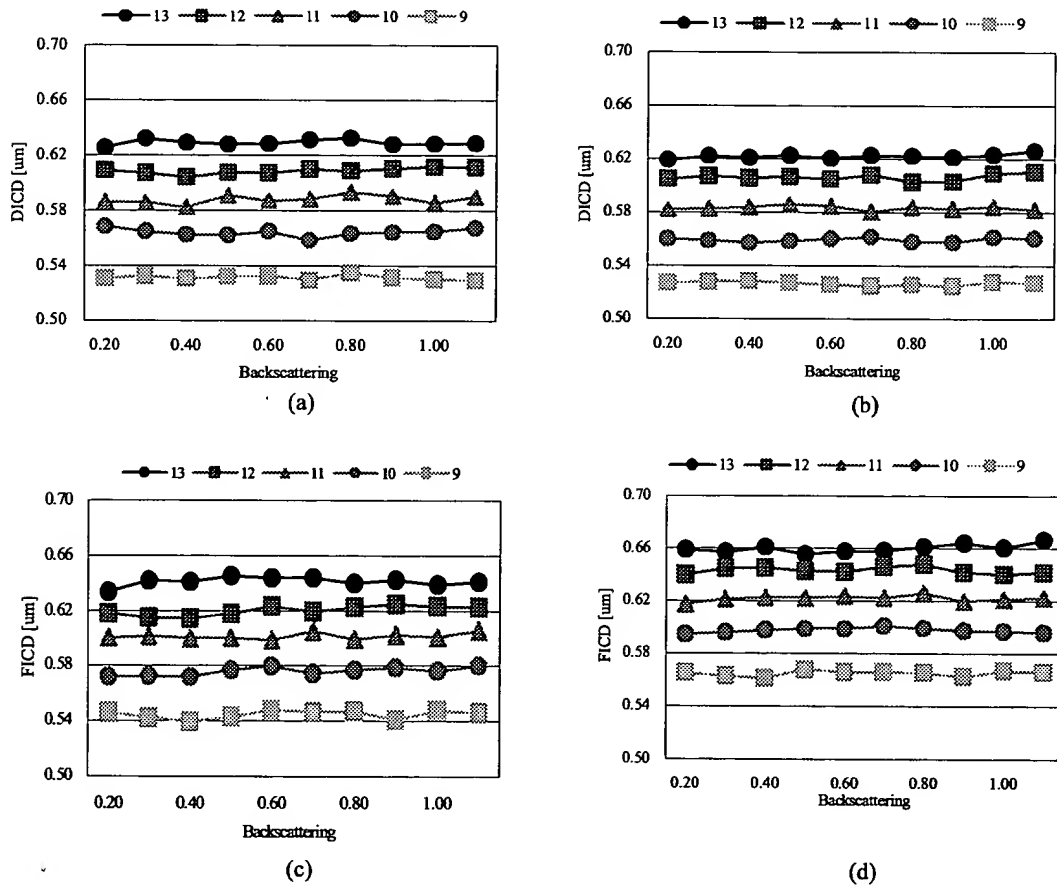


Fig 2. Dose margin range from 9  $\mu\text{C}/\text{cm}^2$  to 13  $\mu\text{C}/\text{cm}^2$  relationship between backscattering ratio and Cr film thickness.

(a) Cr 400  $\text{\AA}$ , DICD, (b) Cr 1000  $\text{\AA}$ , DICD, (c) Cr 400  $\text{\AA}$ , FICD, and (d) Cr 1000  $\text{\AA}$ , FICD.

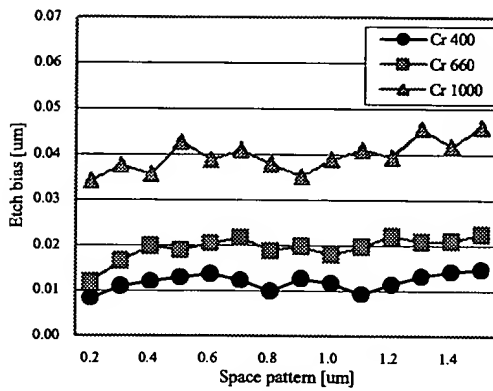


Fig 3. Comparison of etching linearity for three samples.

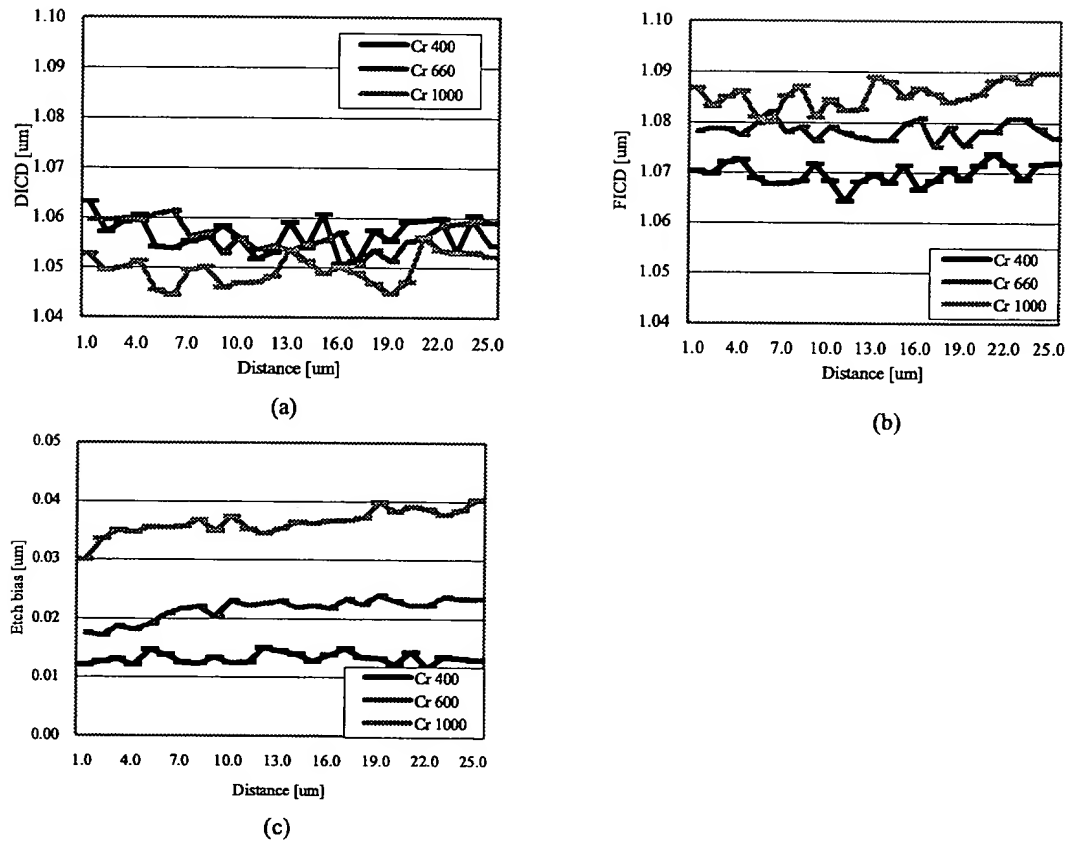


Fig 4. Relationship between backscattering width and Cr film thickness.

(a) DICD, (b) FICD, and (c) Etch bias (FICD-DICD).

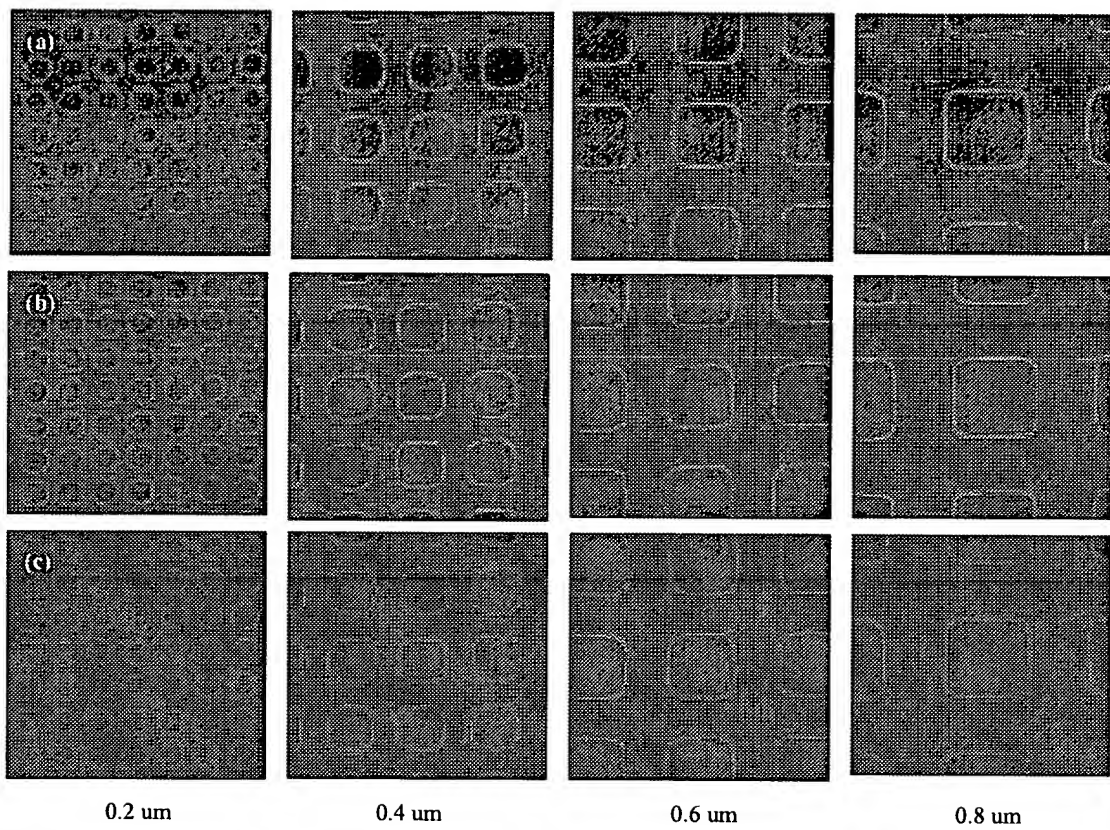


Fig 5. Pattern fidelity. (a) Cr 400 Å, (b) Cr 660 Å, and (c) Cr 1000 Å.